Heteroatom Bridged Tetrathiafulvalenes

Narcis Avarvari

Heteroatom Bridged Tetrathiafulvalenes

Narcis Avarvari*,[a]

[a] Dr. N. Avarvari

MOLTECH-Anjou, UMR 6200, CNRS, UNIV Angers, 2 bd Lavoisier, 49045 ANGERS Cedex, France. E-mail: narcis.avarvari@univ-angers.fr; http://moltech-anjou.univ-angers.fr

ORCID
Narcis Avarvari: 0000-0001-9970-4494

Abstract: Tetrathiafulvalene (TTF) derivatives are the most representative electroactive precursors for the preparation of crystalline conducting materials. The occurrence of mixed valence states, through electron delocalization, and strong intermolecular interactions are important prerequisite to account for high electronic conduction in the solid state and dimensionality of the material. In this respect the modulation of through space or through bond intramolecular electron communication can be efficiently achieved in heteroatom bridged bis(TTF) derivatives. Moreover, the bridging heteroatoms can engage, depending on their nature, in intermolecular interactions in the solid state. In this Review we focus on flexible and rigid bis(TTF) derivatives formulated as $X(TTF)_2$ and $X_2(TTF)_2$ (X = Si, Ge, Sn, P, Sb, S, Se, Te) thus containing one or two bridges in *ortho* position. A special attention is given to the solid state structures of these precursors and their oxidized species, their electrochemical behavior, reactivity, role of the heteroatom in the establishment of intramolecular mixed valence and intermolecular interactions, and the conducting properties.

1. Introduction

The occurrence of mixed valence states, as a consequence of electron delocalization, in charge transfer complexes and radical cation salts based on tetrathiafulvalene (TTF) derivatives is an important feature to favoring interesting conducting properties.[1–3] In this respect, promoting intramolecular though-space or through-bond electronic communication between at least two TTF units represents a valuable strategy to access multi-redox stage systems and thus to enhance the probability to obtain mixed valence species.[4,5] Moreover, the higher extent of the charge delocalization is in principle favorable to decreasing the intermolecular Coulomb repulsion and to increasing the orbital overlap between open shell species in the solid state. It is therefore not surprising that several dimeric or oligomeric TTF families with various linkers between the redox active units have been reported over the years in the literature, such as directly linked dimeric TTFs,[6] bis-TTFs with conjugated[7] or aliphatic[8–11] spacers, derivatives containing aromatic[12–16] or heteroaromatic[17–19] bridges, transition metal fragments[20] or

metal clusters[21–24] coordinated by at least two TTF ligands, or double bridged tetrathiafulvalenophanes.[25] Of particular interest in this respect are the bis- and tris-TTF donors with the TTF units bridged by heteroatoms as they can provide, beside usually convenient and easily generalizable syntheses, extra-functionalities such as additional X···Chalc or X···X (X = heteroatom) intermolecular interactions, conjugation paths between the redox active moieties, further reactivity or coordination of transition metals. In the case of dimeric TTFs a single heteroatomic bridge provides the flexible series of donors formulated as $X(TTF)_2$, while the connection through two linkers affords the rigid dimeric derivatives $X_2(TTF)_2$ (X = heteroatom) (Scheme 1). For the tris-TTF compounds the only reported examples are those of tertiary phosphines of $P(TTF)_3$ type.[26–28]

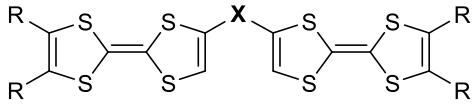

$X(TTF)_2$

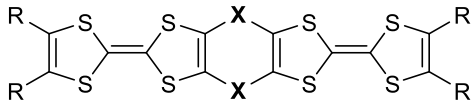

$X_2(TTF)_2$

Scheme 1. Flexible and rigid bis(TTF) donors containing heteroatom based linkers.

The heteroatom bridged bis- and tris-TTFs have been previously reviewed in a larger context more than fifteen years ago.[4,5] Since then, this family of functional electroactive precursors has been enriched with examples coming from different research groups including ours. In this review we will first describe the flexible derivatives $X(TTF)_n$ (n = 2, 3) and then the rigid ones containing two bridges, $X_2(TTF)_2$, mainly reported after 2004 by mentioning, however, anterior examples for comparison purposes. A special focus will be given to the solid state structures, electronic communication and conducting properties of these precursors and materials derived thereof.

2. Flexible bis-TTF and tris-TTF derivatives

The first derivatives of $X(TTF)_2$ type reported in the literature were those containing tellurium bridges in the compounds TTF–Te–TTF[29] **1a** and TTF–Te–Te–TTF[30] **2** (Figure 1), serendipitously obtained by treating the TTF tetratelluride tetraanion with *cis*-dichloroethylene and *ortho*-dichlorobenzene, respectively. Then followed the preparation of $S(TTF)_2$ **1b** and $Se(TTF)_2$ **1c** (Figure 1) through a rational strategy involving the lithiation of TTF followed by trapping the resulting anion with di(phenylsulfonyl)sulfide $(PhSO_2)_2S$ and di(phenylsulfonyl)diselenide $(PhSO_2)_2Se_2$, respectively.[31]

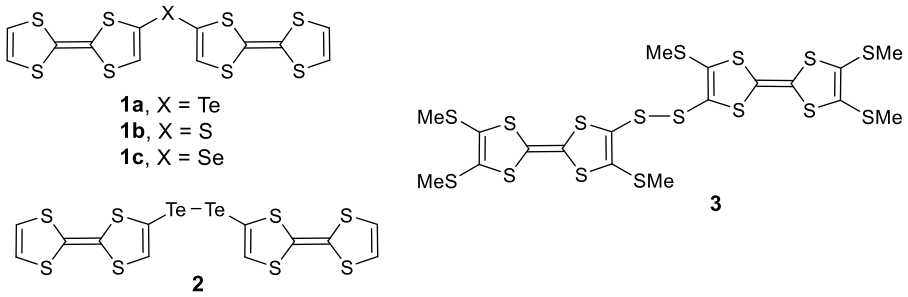

Figure 1. Bis(TTF) compounds with one chalcogen based bridge.

The disulfide bridged bis(TTF) **3** was obtained by taking advantage of the cyanoethyl easily removable protecting group and oxidative coupling of thiolate in the presence of $K_3Fe(CN)_6$.[32] Single crystal X-ray structures have been determined for **1a-b**, **2** and **3**. The TTF units are orthogonal in **1a** and **1b** (Figure 2), with TTF···TTF angles of 89° in both structures, therefore one cannot expect through space electron communication between them.

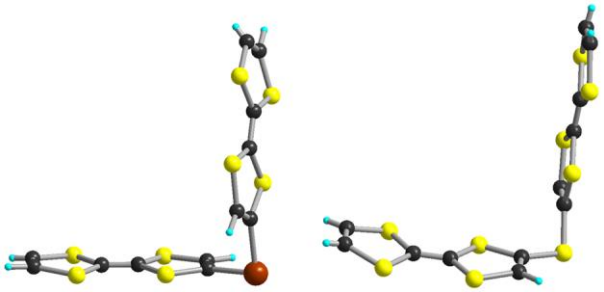

Figure 2. Solid state structures of $Te(TTF)_2$ **1a** (left) and $S(TTF)_2$ **1b** (right).

In the dichalcogenide compounds **2** and **3** the angles between the TTF units are 28° and 39°, respectively, yet they do not overlap at all since the dihedral angles C–X–X–C are 80° for **2** and 69° for **3**, the larger difference than between **1a** and **1b** being imputable to the steric congestion brought by the internal SMe substituents (Figure 3). Again, the lack of TTF···TTF short intramolecular distances are not in favor of through space communication.

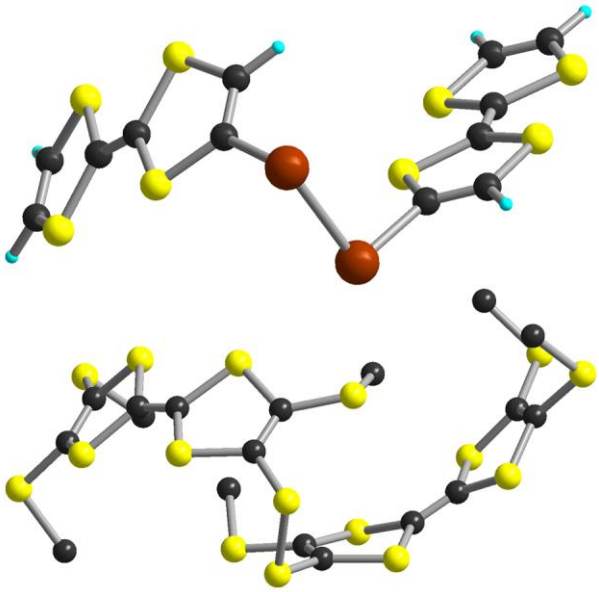

Figure 3. Solid state structures of **2** (top) and **3** (bottom). Hydrogen atoms have been omitted for clarity in **3**.

Although **1a-c** shown splitting of the first oxidation wave in two monoelectronic processes, extended Hückel calculations suggest that through bond communication between the redox active units is very weak in such flexible dimers,[26] and thus the sequential generation of radical cation and dication species is likely due to intramolecular Coulombic repulsions. This analysis was extended to the ditelluride compound **2**[33] and confirmed in the case of **3** by the presence of only two oxidation processes indicative of the concomitant oxidation of both TTF in radical cation and then dication species. While semiconducting behavior has been reported for neutral **2**, very likely thanks to the numerous intermolecular S···S and Te···S short contacts,[33,34] no radical cation salts based on these donors have been reported, but only charge transfer (CT) complexes of **1a** and **2** with TCNQ.[34] Particularly interesting is the CT complex **2**·TCNQ, showing a room temperature conductivity of 0.3 S cm^{-1} and semiconducting behavior, which has been structurally characterized.[35] Now the TTF units within the dimer are arranged in parallel planes, with a C–Te1–Te2–C angle of 91°, indicating that intramolecular TTF···TTF interactions are very weak. Although not discussed in the initial report,[35] the analysis of the central C=C and C–S bonds in TTF indicate that Te2-TTF is more oxidized than Te1-TTF, which is also suggested by the formation of TCNQ stacks, running along *c*, enveloped by Te2-TTF donors in lateral interaction (Figure 4).

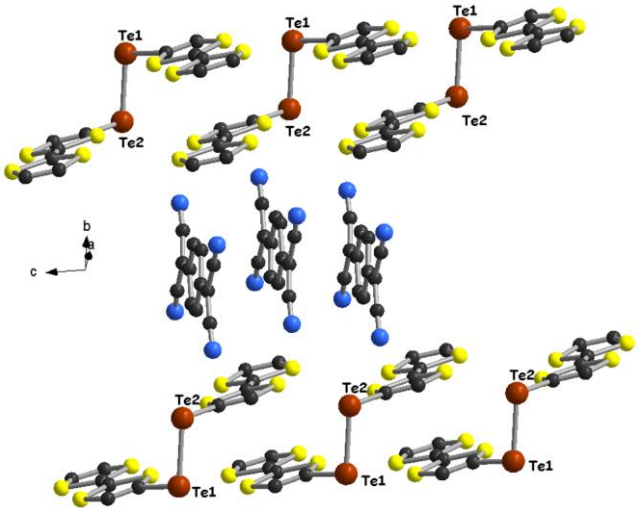

Figure 4. Solid state structure of **2**·TCNQ. Hydrogen atoms have been omitted for clarity.

S···S intermolecular distances between Te1-TTF and Te2-TTF overlapping approximately along (*a*+*b*) range between 3.55 and 3.65 Å, yet no infinite TTF···TTF stacks form along this direction, but tetrameric motifs Te2Te1Te1Te2 involving TTF units from four different molecules (Figure 5). Te atoms are involved as well in short Te···S, Te···N and Te···Te contacts along *c* and approximately (*a*+*b*) and (*a*-*b*), respectively, thus emphasizing the interest of such derivatives to promote original solid state architectures. Clearly, the potential of these chalcogen bridged TTFs for the preparation of conducting materials is underexploited.

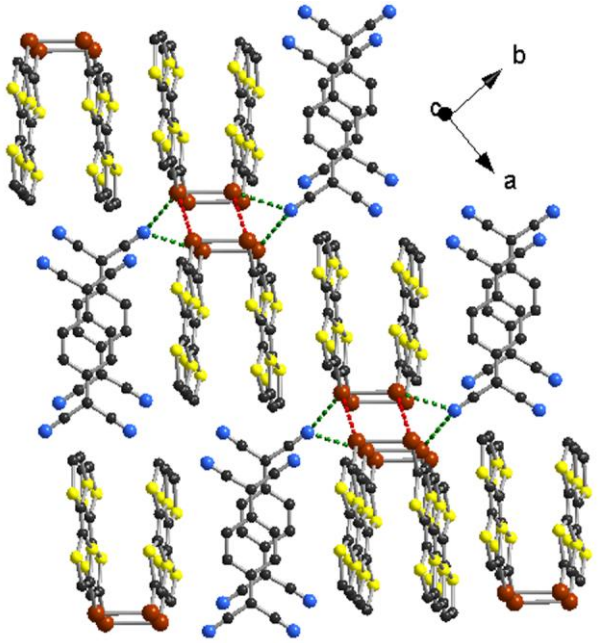

Figure 5. Solid state structure of **2**·TCNQ. Te···Te (3.99 Å) and Te···N (3.22 and 3.49 Å) short contacts are emphasized in dashed red and green lines, respectively. Hydrogen atoms have been omitted for clarity.

Mono- and disilicon bridges bis(TTFs) **4** and **5** (Figure 6), prepared by lithiation of TTF precursors followed by quenching of the monolithiated TTF with dichloro-dimethylsilane and dichloro-tetramethyldisilane, respectively, have been reported by Fourmigué et al. (**4a-b**)[36] and Guyon et al. (**5**).[37]

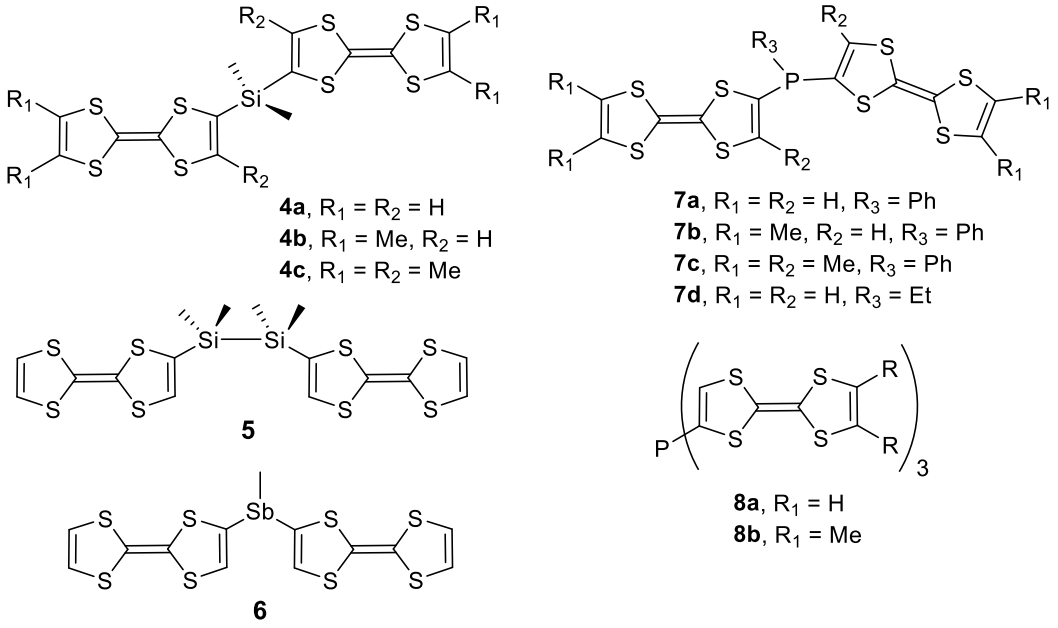

Figure 6. Bis(TTF) compounds with Si, Sb and P bridges and tris(TTF) phosphines.

Single crystal X-ray structures have been determined for compounds **4a** and **5**. The TTF units are almost perpendicular to each other in **4a**, with a dihedral angle of 77° between the two mean planes, while in **5** they are anti-parallel, the dihedral angle amounting at 180° (Figure 7). The shortest S···S intramolecular distance between the two TTF in **4a** is 4.19 Å, much larger than the sum of the van der Waals radii of two sulfur atoms.[38,39]

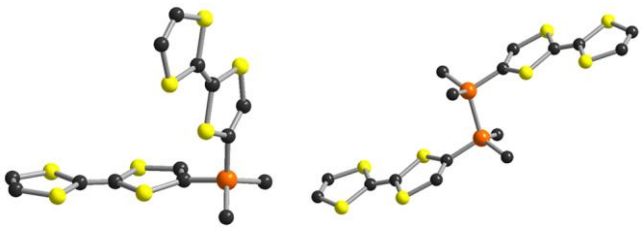

Figure 7. Solid state structures of **4a** (left) and **5** (right). Hydrogen atoms have been omitted for clarity.

While compounds **4a-c** show sequential oxidation of the TTF units in radical cation and then dication,[36] the mono-electronic processes being separated by about 100 mV, in the disilicon bridged compound **5** the oxidation of the redox active units arise concomitantly,[37] indicating negligible electron communication between TTFs. In order to explain the difference in the electrochemical behavior of compounds **4a** and **5**, DFT calculations have been performed. As expected HOMO and HOMO–1 are

the out-of-phase and in-phase combinations of the $HOMO_{TTF}$, whereas, interestingly, the LUMO in **4a** connects the two TTFs through the $SiMe_2$ bridge, while in **5** the disilicon bridge is not involved in the LUMO (Figure 8).

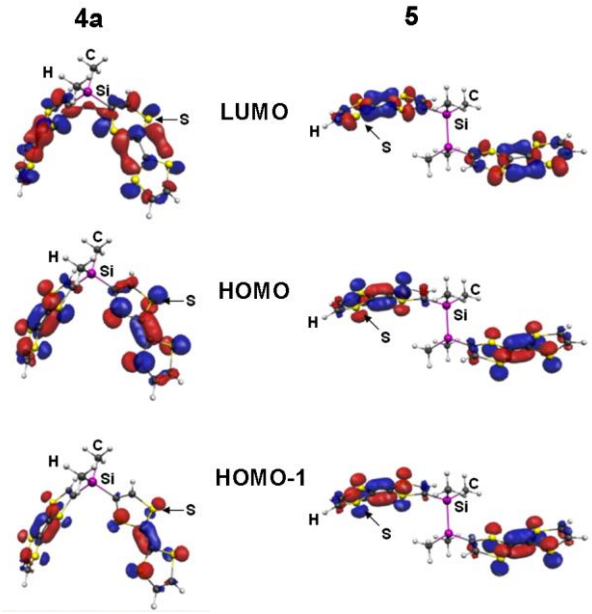

Figure 8. Frontier orbitals of **4a** and **5**. Solid state structures of **4a** (left) and **5** (right). Adapted from ref. [37] with permission of The Royal Society of Chemistry.

It was thus concluded that, in spite of the long intramolecular S···S distances observed in the structure of **4a**, sizeable through-space interaction between the two TTF units take place thanks to the $SiMe_2$ bridge. Note that in the Hg bridged analogue of **4a**, simultaneous oxidation of both TTFs was observed, very likely because of the linearity imposed by the linker.[36]

The use of an antimony linker to connect two TTFs provided compound **6**,[40] following the report of the first examples of TTF stibines.[41] Besides the bridging role, the interest to introduce Sb atoms in the structure of TTF precursors relies on the propensity of antimony to engage in intermolecular Sb···Sb[42] and Sb···S interactions,[41,43,44] thus opening new opportunities to access original architectures in the solid state. The single crystal X-ray structure of **6** shows perpendicular TTF units belonging to the same donor, with a dihedral angle of 88° between them. Worth noting is the establishment of two short Sb···S intermolecular contacts, amounting at 3.59 and 3.73 Å (Figure 9), which complement the classical S···S interactions. As in the case of the other flexible derivatives $X(TTF)_2$ with a single heteroatomic discussed so far, compound **6** shows sequential oxidation in radical cation and dication through reversible one-electron processes, suggesting electronic communication thanks to the MeSb bridge. The first oxidation potential is even slightly cathodically shifted compared to TTF, indicating better electron donor ability for **6** than for TTF.

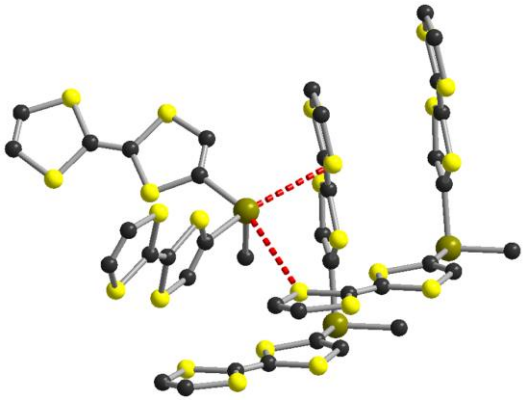

Figure 9. Solid state structure of **6**. Sb···S short contacts (3.59 and 3.73 Å) are highlighted in dashed red lines. Hydrogen atoms have been omitted for clarity.

No radical cation salt or CT complexes have been described so far with this promising donor.

Not surprisingly, the largest family of $X(TTF)_n$ (n = 2, 3) derivatives is the one containing phosphorus bridges (Figure 6), since their formation is easily monitored by ^{31}P NMR spectroscopy, diverse halogenated phosphine precursors are available and they can be used as electroactive ligands towards transition metal centers.[20] Their synthesis takes advantage of the convenient reaction of lithiated TTFs with halophosphines PBr_3 or $RPCl_2$. Accordingly, bis(TTF) phosphines **7a-d** and tris(TTF) phosphines **8a-b** have been prepared by this strategy, the first reported one being $P(TTF)_3$ **8a** described by Fourmigué,[26] followed by the series of bis(TTFs) **7a-c**[36] and the tris(TTF) **8b**[28] by the same author, and, finally, the bis(TTF) **7d** reported by DiSalvo and Lee, used as ligand to decorate the W_6S_8 core.[23] Both tris(TTF) phosphines have been characterized by single crystal X-ray analysis. While **8a** crystallized in the monoclinic space group *C*2/c with one independent molecule in the asymmetric unit,[26] in **8b** the C_3 symmetry of the molecule has been transposed to the crystal level, as the P atom lies on a C_3 symmetry axis of the trigonal space group *R*3c, thus only one third of the molecule being independent in the asymmetric unit (Figure 10).[28]

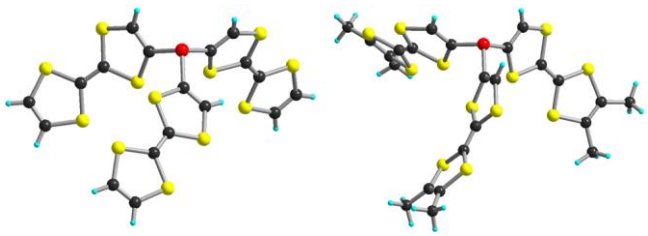

Figure 10. Solid state structures of **8a** (left) and **8b** (right).

The dihedral angles between the TTF units belonging to the same donor are in the range 69.9°-72.3° for **8a** and 66.4° for **8b**, the three TTF being equivalent in the latter. The only bis(TTF) phosphine structurally characterized is **7b**.[28] Comparable to the tris(TTF) compounds, the intramolecular dihedral

angle between the TTF units is 65°, and in the packing the donors stack along the *b* direction in a crisscross manner (Figure 11).

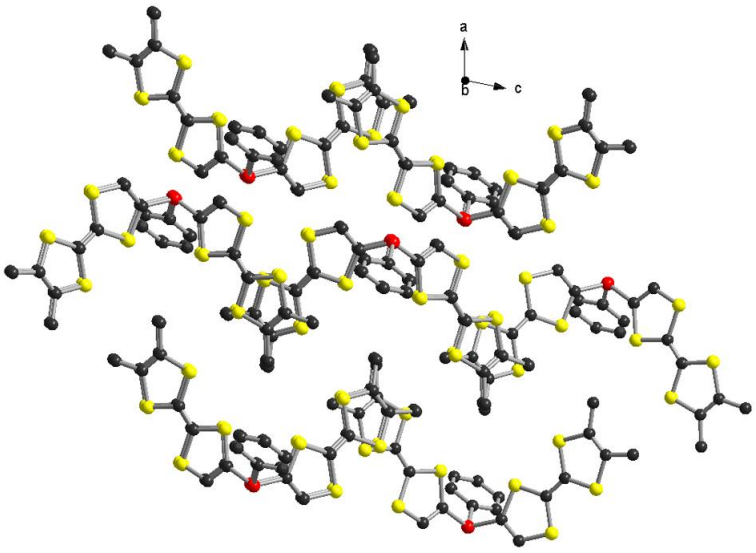

Figure 11. Packing along *b* in the solid state structure of **7b**. Hydrogen atoms have been omitted for clarity.

Cyclic voltammetry measurements show stepwise oxidation in monocation and dication for **7a-c** and monocation, dication and trication for **8a-b** with ΔE value of approx. 100 mV between the successive monoelectronic processes, clearly indicating electronic communication between the redox active units. Interestingly, EPR measurements on the radical monocation species of **7a-b** and **8a-b** chemically or electrochemically generated show hyperfine couplings of the radical with all the TTF protons, a strong proof of the intramolecular electron delocalization between the two or three TTFs at the EPR timescale.[27] The coordination chemistry of these electroactive phosphines is underexploited at the difference with that of mono-TTF phosphines or mono-TTF diphosphines,[20,45–47] the latter having provided crystalline radical cation salts as well.[48] To date, only the bis(TTF) phosphines **7b** and **7d** have been used as ligands to coordinate the apical positions of the Re_6Se_8[21,49] and W_6S_8[23] clusters. Electrochemical measurements performed on the former are in agreement with concomitant oxidation of the twelve TTF units in radical cations and then dications, yet no crystalline forms of these oxidized species has been isolated in order to investigate their solid state properties.

3. Rigid bis-TTF derivatives

The precursors belonging to this family contain two heteroatomic bridges connecting two TTF type donors in the *ortho* positions, excepting the bis(TTF)-selenophene **9** where the TTF units are fused to a central selenophene (Figure 12).

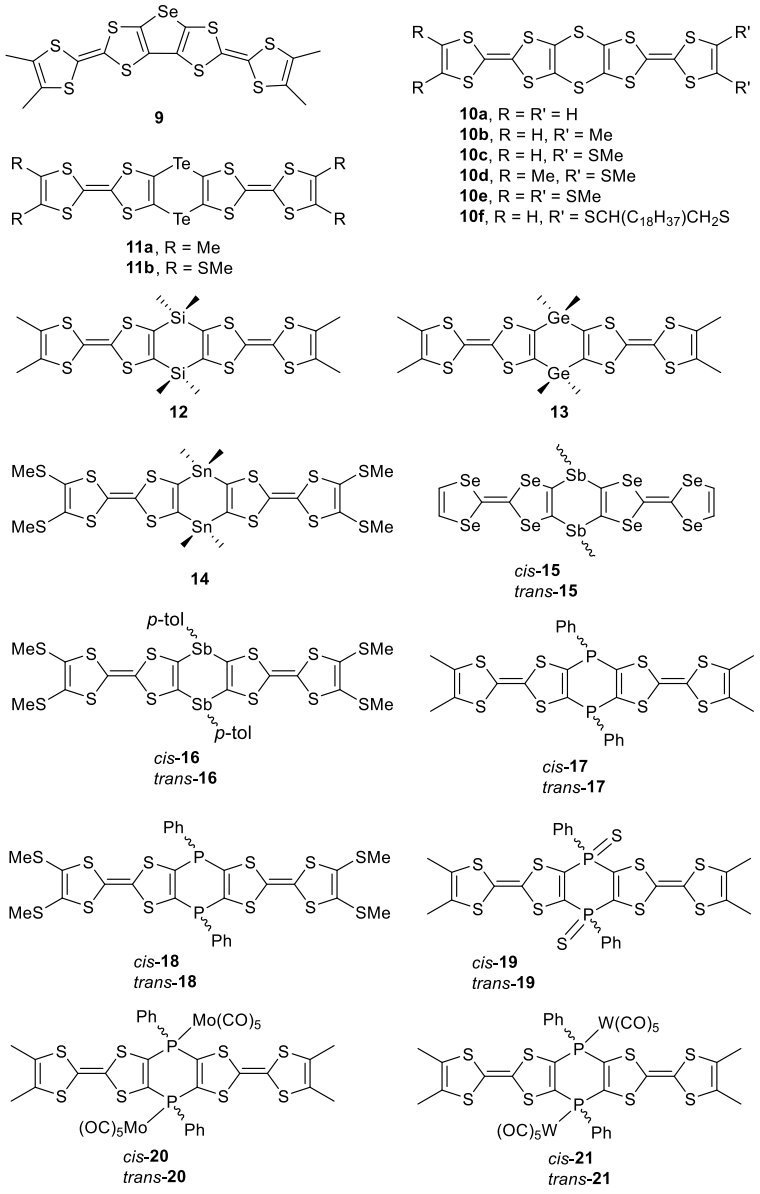

Figure 12. Rigid bis(TTF) compounds.

One can identify two distinct periods in the development of the rigid bis(TTF) precursors represented in Figure 12. Accordingly, the chalcogen bridged compounds **9**-**11** and derived charge transfer and radical cation salts were reported in the middle of the 90's thanks to the pioneering works of Becker and Bernstein, followed by a lull probably due to synthetic issues in the preparation of the donors. Then a revival of the field started in 2004 with the report on the diphosphinine compound **17**,[50] which motivated further activity from three different groups including ours.

The bis(TTF)-selenophene **9** was serendipitously obtained by the lithiation of *ortho*-DM-TTF and trapping of the dilithio TTF salt with $(PhCC)_2Se$.[51] Cyclic voltammetry measurements indicate stepwise one-electron oxidation of the TTF units up to tetracation, the last two processes being hardly reversible (Table 1). A very large separation of ΔE = 160 mV was observed between the first two oxidations,

indicating an excellent electron communication between the two TTFs through the central selenophene ring.

Table 1. Electrochemistry data for compounds **9-18**. All potential values were converted to vs. SCE as reference electrode in order to facilitate the comparison.

Compound	Bridging element	$E^1_{1/2,ox}$	$E^2_{1/2,ox}$	$E^3_{1/2,ox}$	$E^4_{1/2,ox}$	Ref.
9[a]	Se	0.38	0.54	0.91[b]	0.95[b]	[51]
10a[a]	S	0.45	0.65	0.87		[52]
10b[a]	S	0.41	0.62	0.86		[52]
10c[a]	S	0.47	0.73	0.87		[52]
10d[a]	S	0.45	0.74	0.85		[52]
10f[c]	S	0.38	0.55	0.74		[53]
11a[a]	Te	0.46	0.81			[55]
11b[a]	Te	0.55	0.82			[56]
12[c]	Si	0.25	0.37	0.79		[58]
13[c]	Ge	0.22	0.33			[58]
14[a]	Sn	0.45	0.71			[59]
15[a]	Sb	0.23	0.59			[40]
16[a]	Sb	0.39	0.73			[60]
17[a]	P	0.45	0.57	0.95	1.07	[61]
18[a]	P	0.56	0.62	0.94	1.02	[62]

[a] in C_6H_5CN; [b] ill defined; [c] in CH_2Cl_2.

The single crystal structure of **9** shows full planarity of the donor which engages in several intermolecular S···S and Se···S short contacts, the latter ranging between 3.71 and 3.91 Å, as highlighted in Figure 13.

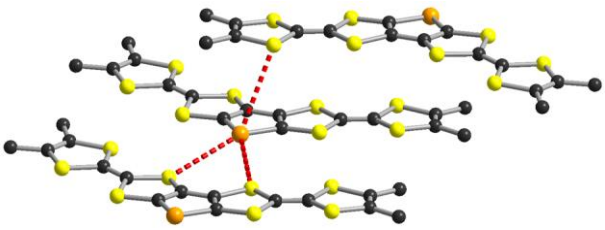

Figure 13. Solid state structure of **9** with an emphasis on the short intermolecular Se···S contacts (in red dashed lines). H atoms have been omitted.

A charge transfer complex of this donor with TCNQ shows a room temperature conductivity of 30 S cm^{-1} in average for compressed pellets as no single crystals were obtained.[51] Unfortunately no further work was dedicated to this very interesting donor.

The bis(TTF) dithiin derivatives **10a-d**[52] and **10f**[53] have been prepared by a multistep procedure involving as final step the phosphite mediated cross coupling of diversely substituted TTF-dithiine-dithiolones **22** with dithiothiones **23**, while the symmetrical derivative **10e**[54] was obtained by a double

cross coupling between dithiine-bis(dithiolone) **24** and the bis(thiomethyl)-dithiothione half (**23** with R' = SMe) (Figure 14).

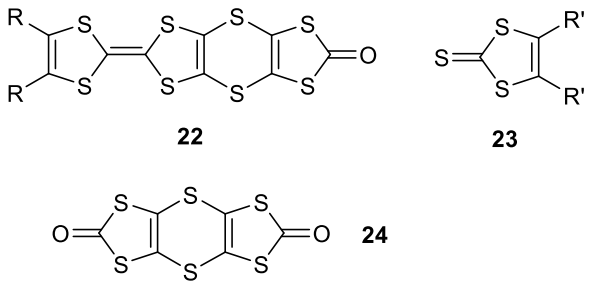

Figure 14. Intermediates in the synthesis of **10a-f**.

According to the cyclic voltammetry measurements of compounds **10** (Table 1) the first two oxidation processes, which could be attributed to the sequential formation of radical cation and then dication, are separated by 170 – 290 mV, suggesting strong intramolecular electron communication, while the generation of tetracationic species occurs in one two-electron process. Note that the amphiphilic compound **10f** has been synthesized with the objective to prepare conducting Langmuir-Blodgett films.[53] While no structural characterization was reported on neutral **10**, only one crystalline conducting material has been characterized by single crystal X-ray diffraction. It concerns the CT complex of **10c** with TCNQ,[52] which consists in two donors and one acceptor in the asymmetric unit. The authors mentioned a charge transfer degree for TCNQ of 0.6 based on the infrared CN vibration frequency, corresponding to a mean oxidation state of +0.15 per TTF unit, with the compound showing semiconducting properties, with a room temperature conductivity of 6 S cm^{-1} in compressed pellet. However, although not discussed in the article, the C=C central distances of TTF, i.e. 1.43 and 1.28 Å, indicate charge localization, with one charge rich and one charge poor donors. Interestingly, while the TTF units are planar, the donors adopt an overall V shape, with dihedral angles of 56° between the TTF mean planes around the central S···S axis of the dithiin ring. The donors stack along the *b* axis and interact laterally along *a*, while along *c* there is alternation of donor and acceptor slabs (Figure 15), with numerous short S···S intermolecular contacts.

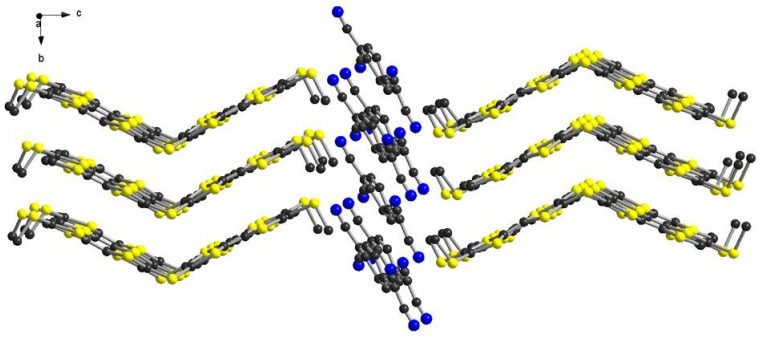

Figure 15. Packing in the *bc* plane in the structure of (**10c**)$_2$•TCNQ. H atoms have been omitted.

The ditellurin compounds **11a-b** have been prepared by reaction of the Me or SMe TTF dilithio salts with $(PhCC)_2Te$.[55,56] Intriguingly, they show only two oxidation processes (Table 1), which could correspond to the formation of dication and tetracation species, respectively, since the ΔE values are relatively large. No further more detailed electrochemical studies have been reported on these donors. Both donors have been structurally characterized by single crystal X-ray diffraction. They show an unusual sombrero-like conformation, with strong folding around the Te···Te axis of 67° (**11a**) and 64° (**11b**), and around the S···S hinges of the internal dithiol rings with values of the respective dihedral angles of 33° (**11a**) and 30° (**11b**) (Figure 16).

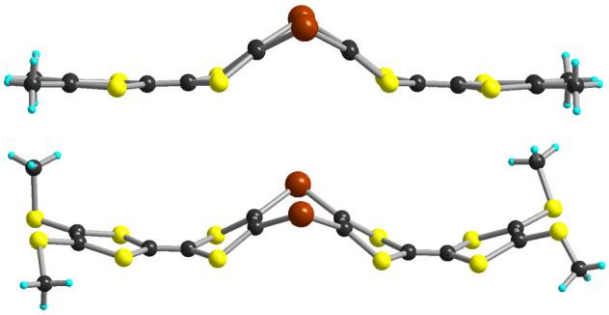

Figure 16. Solid state structures of **11a** (top) and **11b** (bottom).

A CT complex of **11a** with the 2,5-dimethyltetracyano-*p*-quinodimethane (DMTCNQ) acceptor with a room temperature conductivity of 6 S cm^{-1} was briefly mentioned.[55] Strangely, the only radical cation salts so far reported contains the oxidized donor **11a** and the anion $[Au(CN)_2]^-$ in a ratio 1:0.42 and was serendipitously obtained by electrocrystallization of propyleneditelluro-TTF-dimethyl donor, which obviously decomposed and fused during the process to provide **11a**.[57] The salt is semiconducting with room temperature conductivities of 1-10 S cm^{-1} and small activation energies.

Group XIV bridged bis(TTF) donors **12**-**14** (Figure 12) were described more than ten years later. Compounds **12** and **13** with $SiMe_2$ and $GeMe_2$, reported by our group,[58] were prepared by reaction of dilithio salt of dimethyl-TTF (DM-TTF) with the corresponding dichloride precursors, while **14** was obtained through a similar strategy by Hasegawa and Mazaki from bis(methylthio)-TTF (BMT-TTF) and Me_2SnCl_2.[59] Interestingly, while compounds **12** and **13** show sequential reversible one-electron oxidation into radical cation and dication species, the tin bridged precursor **14** is two-electron oxidized to reach directly the dication (Table 1). The three compounds provided suitable single crystals for X-ray measurements. They show similar chair-like conformations in the solid state, with planar central six-membered rings and folding around the S···S hinges of the internal dithiol rings of 20° for **12**-**13** and 16° for **14** (Figure 17).

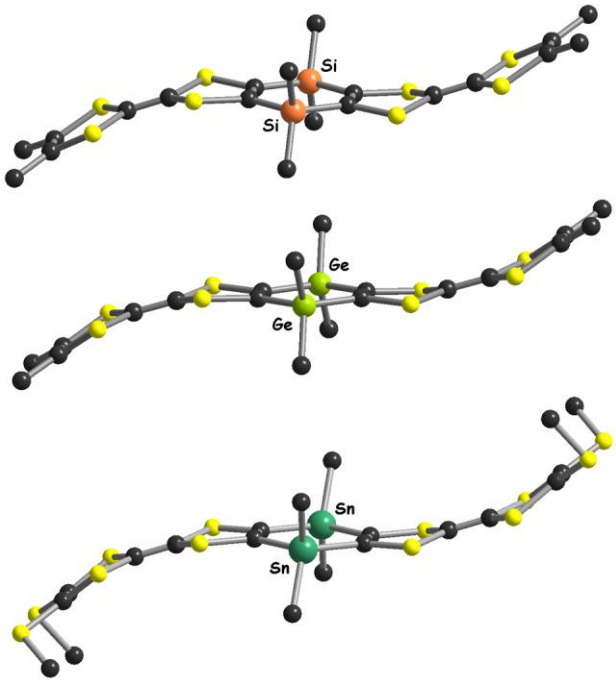

Figure 17. Solid state structures of **12** (top), **13** (middle) and **14** (bottom).

DFT calculations have been performed on the three compounds and the optimized geometries are in excellent agreement with the experimental ones observed in the solid state. Worth mentioning are the frontier orbitals as HOMO and HOMO-1 consist of the antisymmetric and symmetric combination of the π TTF orbitals, while the LUMO develops over the central six-membered ring and consists in the in-phase combination of σ^* EMe_2 (E = Si, Ge, or Sn) and vinyl π^* orbitals (Figure 18 for **12**).

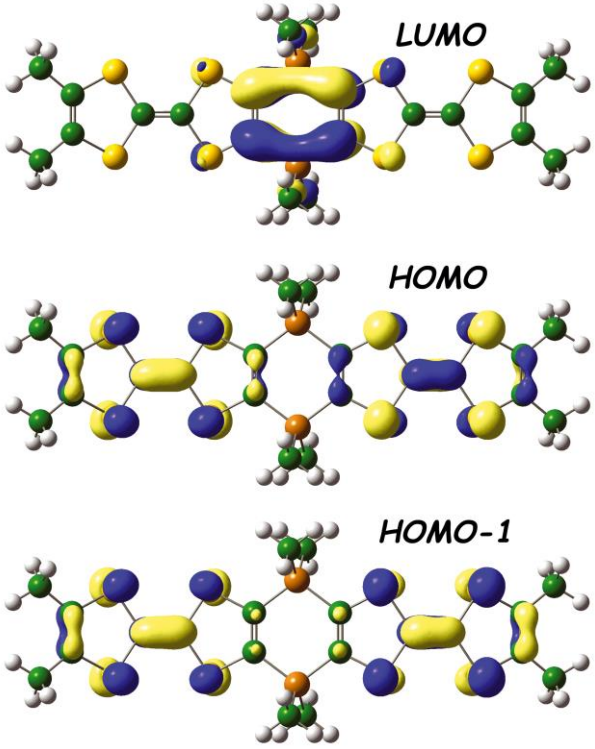

Figure 18. Frontier orbitals of **12**. The energies at the DFT/B-P86/SV (P) level are: -4.735 eV (HOMO-1), -4.653 eV (HOMO) and -1.170 eV (LUMO). Adapted from ref. [58]; Copyright 2007, John Wiley and Sons.

The energy difference between HOMO and HOMO-1 decreases in the order Si > Ge > Sn, with ΔE values of 82 meV for **12**, 60 meV for **13**, while they are practically degenerated in **14**, this feature being consistent with the observation of stepwise one-electron oxidation to radical cation and dication for **12** and **13** and two-electron oxidation to dication for **14** (see Table 1). The occurrence of stable radical monocations in the case of chemical and electrochemical oxidation of **12** and **13** has been unambiguously demonstrated by solution EPR measurements. Accordingly, the EPR spectra of the radical monocations show a hyperfine structure corresponding to the coupling of the unpaired electron with 12 equivalent protons from the four lateral methyl groups, indicating electron delocalization over both TTF units at room temperature at the EPR time scale (Figure 19 for **12**).

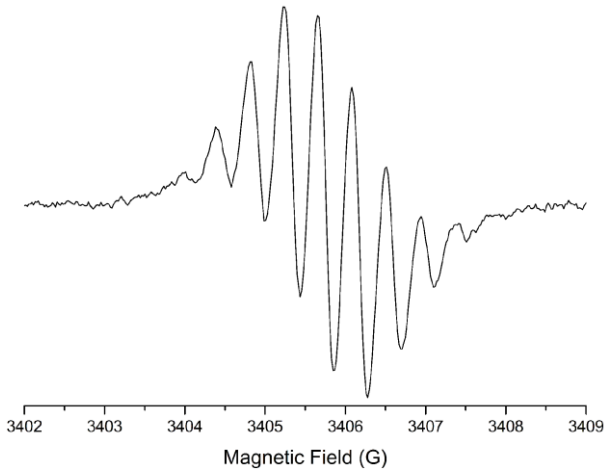

Figure 19. EPR spectrum of **12**$^{+\cdot}$ (CH_2Cl_2, 1 equiv. $NOSbF_6$, ν = 9572 MHz, T = 300 K); g_{iso} = 2.0081, A_{iso} = 0.42 G. Reproduced from ref. [58]; Copyright 2007, John Wiley and Sons.

Crystalline charge transfer complexes formulated as [**12**]·1/2[TCNQ]·1/2[$TCNQF_4$], [**13**]·[TCNQ] and [**14**]·[$TCNQF_4$]$_2$ have been obtained with this series of donors, in line with their electrochemical behavior, since in the two former the donors are oxidized into radical monocations,[58] while in the latter the dication has been generated.[59] The CT complexes of **12** and **13** are isostructural and contain fully planar oxidized donors which interact along the *a* axis in the *ac* plane (Figure 20 for [**13**]·[TCNQ]).

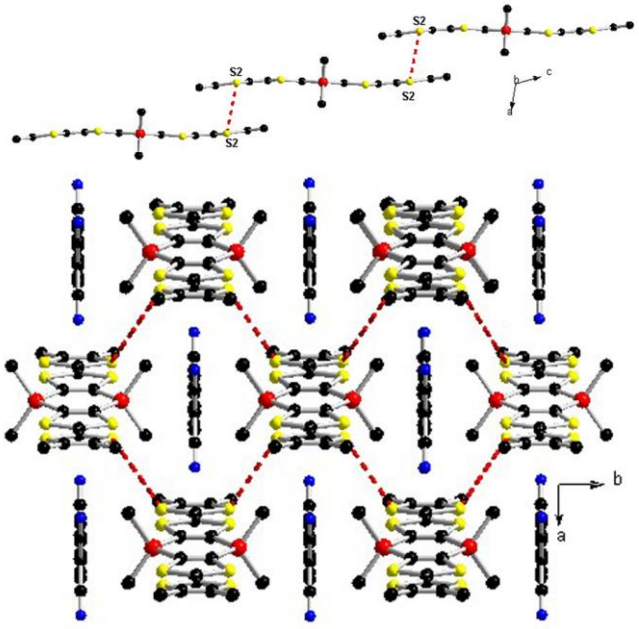

Figure 20. Packing of donors along *a* in the structure of [**13**]·[TCNQ] (top). Intermolecular distances [Å]: S2···S2$^{\#}$ 3.823 Å. Symmetry operator for generating equivalent atoms: ($^{\#}$) 1-x, y, 1-z. Packing in the *ab* plane (bottom) with an emphasis on the short intermolecular S2···S2 (0.5-x, 0.5-y, 1-z) distance of 3.990 Å. Adapted from ref. [58]; Copyright 2007, John Wiley and Sons.

Since the TTF units are identical as they correspond each other through a C_2 symmetry axis along the E···E hinge, the charge transfer degree is +0.5 per TTF. Single crystal conductivity measurements show semiconducting behavior with room temperature conductivities of 6 10^{-2} S cm^{-1} and 3 10^{-3} S cm^{-1} for the Si and Ge compounds, respectively. An applied hydrostatic pressure of 22 kbar on the latter leads to an increase of the conductivity up to 0.2 S cm^{-1}.[58] Band structure calculations show that there is no band gap between the valence and conduction bands, therefore the semiconducting behavior must result from electron localization.

In the CT complex [**14**]·$[TCNQF_4]_2$ there are two independent donors, each of them in the dicationic state. The central six-membered ring adopts now a boat conformation leading to butterfly shape for the donor, with dihedral angles of 131° and 139° around the Sn···Sn hinges for the two independent molecules (Figure 21 shows one of the two independent donor molecules).[59]

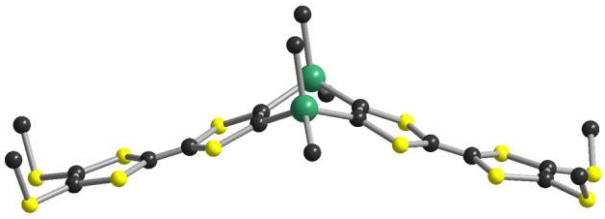

Figure 21. One independent dicationic donor molecule in the solid state structure of [**14**]·$[TCNQF_4]_2$. H atoms have been omitted.

The electronic conductivity of this CT complex has not been reported, but one can suppose an insulating character, as in the packing there is dimerization of the donors and the acceptors. No radical cation salts based on donors **12**-**14** have been reported so far.

In the pnictogen series only antimony, in compounds **15**-**16**, and phosphorous based bridges, in the series of 1,4-diphosphinines and derivatives **17**-**21**, have been used to doubly connect in *ortho* position two redox active units. Worth noting is that **15** is the only tetraselenafulvalene (TSF) derivative within the whole series. It was synthesized by lithiation of TSF and then reaction with $MeSbI_2$, and was isolated as *cis* and *trans* isomers in a ratio of approximately 1/5 after column chromatography.[40] Interestingly, compound **16** was prepared by metathesis reaction of the tin derivative **14** with *p*-$tolSbCl_2$, once again as a mixture of *cis* and *trans* isomers which were separated by size-exclusion gel permeation chromatography (GPC).[60] Here the ratio *cis*/*trans* was 2.5/1 and no interconversion between the two isomers has been observed by heating or cooling. For both antimony bridged derivatives **15** and **16** cyclic voltammetry measurements show two reversible two-electron oxidation processes (Table 1) suggesting that no intramolecular electron communication within the dimer occurs. For both compounds the *cis* and *trans* isomers have been crystallized and their solid state structures present several interesting features. In **15** the central bis(antimony) six-membered ring shows boat

conformation, with dihedral angles of 67° for *cis* and 56° for *trans*, in the latter the bridge being disordered over two positions (Figure 22).

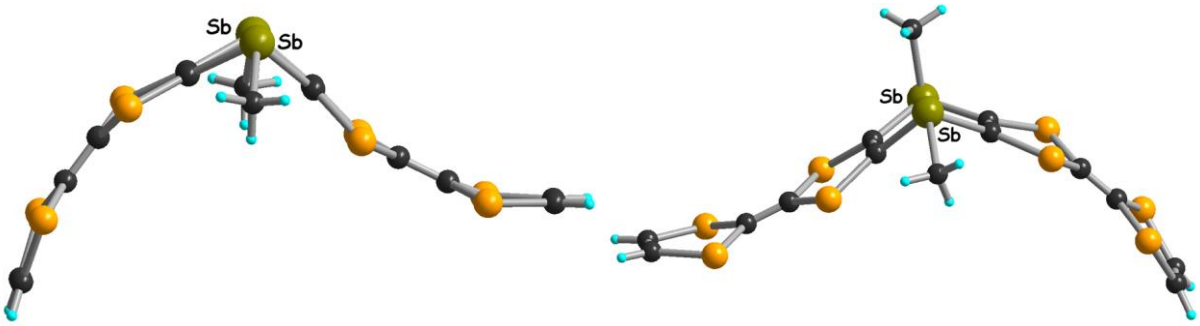

Figure 22. Solid state structures of *cis*-**15** (left) and *trans*-**15** (right). Only the major motif is shown for *trans*-**15**.

Several short intermolecular Se···Se contacts of 3.69-3.81 Å are observed in the structure of *cis*-**15**, yet no particularly short Sb···Sb or Sb···Se distances were noticed. On the contrary, in the *cis* isomer of **16** a remarkably short Sb···Sb distance of 3.65 Å is observed, while the central ring is much less distorted than in *cis*-**15**, the dihedral angle around the Sb···Sb axis being 18° (Figure 23). The tolyl substituents adopt an *endo*/*endo* orientation.

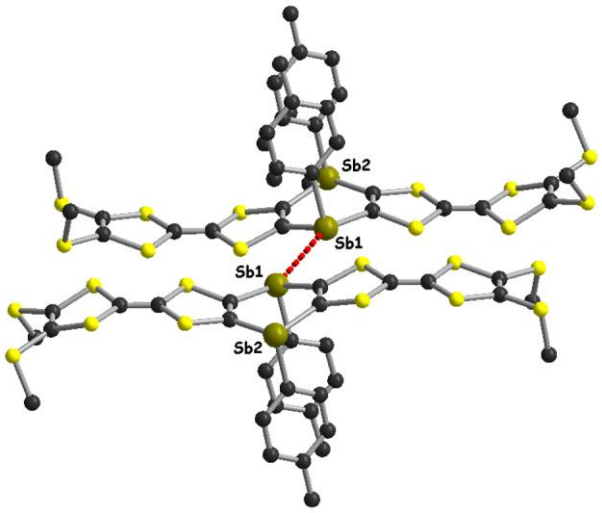

Figure 23. Solid state structure of *cis*-**16** with an emphasis on the Sb···Sb short contact (red dotted line) of 3.65 Å. H atoms have been omitted.

Besides, Sb···S contacts below the sum of the van der Waals radii are also established, thus emphasizing the key role of the heavy pnictogen in the solid state architecture. Interestingly, the *trans* isomer provided two crystalline polymorphs I and II that differ by the folding of the central ring and the orientation of the *p*-tolyl substituents (Figure 24).

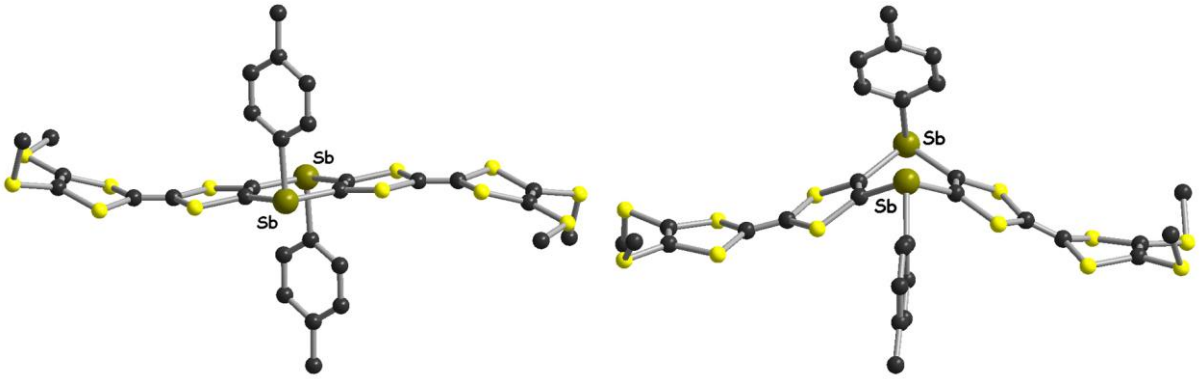

Figure 24. Conformations of *trans*-**16** in the two crystalline polymorphs: I *endo*/*endo* (left) and II *endo*/*exo* (right) with respect to the tolyl substituents. H atoms have been omitted.

Accordingly, in polymorph I with the tolyl substituents in pseudo-axial positions (*endo*/*endo*) the central ring is planar, while in II it adopts a boat conformation with a dihedral angle of 56° around the Sb···Sb axis and tolyl substituents in pseudo-axial and pseudo-equatorial positions (*endo*/*exo*). DFT calculations yielded *cis*-**16** *exo*/*exo*, *cis*-**16** *endo*/*endo* and *trans*-**16** *endo*/*exo* (polymorph II) as energy minima structures, with an energy difference of 9.1 kJ mol^{-1} between the two *cis* conformers in favor of *cis*-**16** *exo*/*exo*. Thus the occurrence of the *endo*/*endo* conformation in the solid state should be the consequence of the packing forces and intermolecular interactions. In agreement with the electrochemistry studies indicating two reversible two-electron oxidation processes, chemical oxidation of **16** with $Fe(ClO_4)_3$ afforded dicationic and tetracationic species characterized by optical absorption spectra.

The last series of rigid dimers concerns the 1,4-dihydro-1,4-diphosphinines **17**-**18** and their phosphorous functionalized derivatives **19**-**21** (Figure 12). The former were synthesized by bis-lithiation of DM-TTF and BTM-TTF followed by reaction with $PhPCl_2$ to provide **17**[61] and **18**,[62] respectively, as a mixture of *cis* and *trans* isomers with the former being the major one. Recrystallization of a *cis*/*trans* mixture of **17** in a ratio 15/1 provided suitable single crystals of *cis*-**17** alone, while in the crystals obtained from a *cis*/*trans* mixture 4/1 of **18** both isomers were present. Interestingly, in *cis*-**17** the Ph substituents adopt an *endo*/*endo* orientation, while in *cis*-**18** they are arranged in *exo*/*exo*, although in both structures the central diphosphinine rings are folded in a boat conformation with dihedral angles of 26° and 39°, respectively (Figure 25).

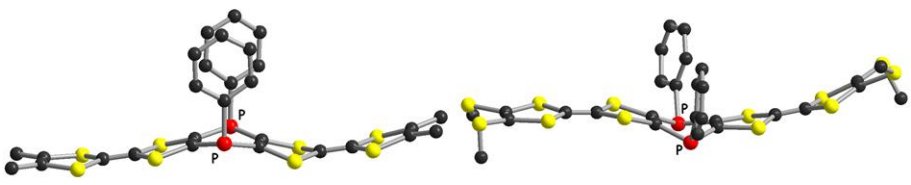

Figure 25. Solid state structures of *cis*-**17** (left) and *cis*-**18** (right). H atoms have been omitted.

In large contrast with the Sb bridged analogues (*vide supra*), cyclic voltammetry measurements on **17** and **18** show four reversible one-electron oxidation processes, with ΔE values of 120 mV and 60 mV between the first two oxidations, i.e. formation of radical cation and then dication, and 120 mV and 80 mV between the last two, corresponding to tris and tetracations, for **17** and **18** respectively (Table 1), thus indicating sizeable electron communication between the two redox active units. According to DFT calculations the *cis* isomer of **17** is slightly more stable than the *trans* one. Nevertheless, the most striking theoretical result concerns the rise of degeneracy between the occupied frontier orbitals with an energy difference of ΔE = 42 meV between HOMO and HOMO-1, the former being the antisymmetric combination of the two TTF π orbitals and the latter the symmetric combination, with a participation of the phosphorus atoms. These results confirm that the double phosphino bridge connects electronically the TTF moieties.[61] A clear proof of this statement was provided by UV-visible spectroelectrochemistry and, especially, EPR spectroelectrochemistry on *cis*-**17**.[63] Accordingly, in the potential range 0.4-0.8 V vs. SCE, the absorption bands at 463 nm and 652 nm are indicative of the presence of TTF radical cation species (Figure 26), suggesting that the most stable form of the dication is a triplet, also in agreement with the results of DFT calculations. Indeed, the triplet state of [*cis*-**17**]$^{2+}$ is 11.7 kcal mol^{-1} lower in energy than the singlet state.

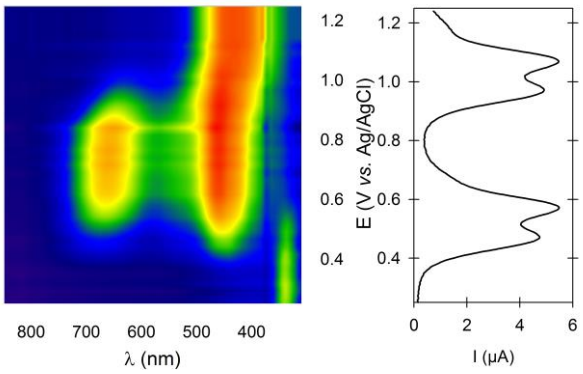

Figure 26. UV-vis spectroelectrochemistry of *cis*-**17**. Reprinted with permission from ref. [63]; Copyright 2009, American Chemical Society.

Outstanding evidence concerning the electron delocalization in [*cis*-**17**]$^{+\bullet}$ has been obtained thanks to EPR spectroelectrochemistry investigations which afforded a spectrum with a hyperfine structure in accordance with a coupling of 0.48 G of the radical with twelve equivalent protons from the four lateral methyl substituents (Figure 27a), further supported by the single hyperfine coupling constant (A_{iso} = 1.32 MHz) detected in the ^{1}H- ENDOR spectrum (inset Figure 27a).[63]

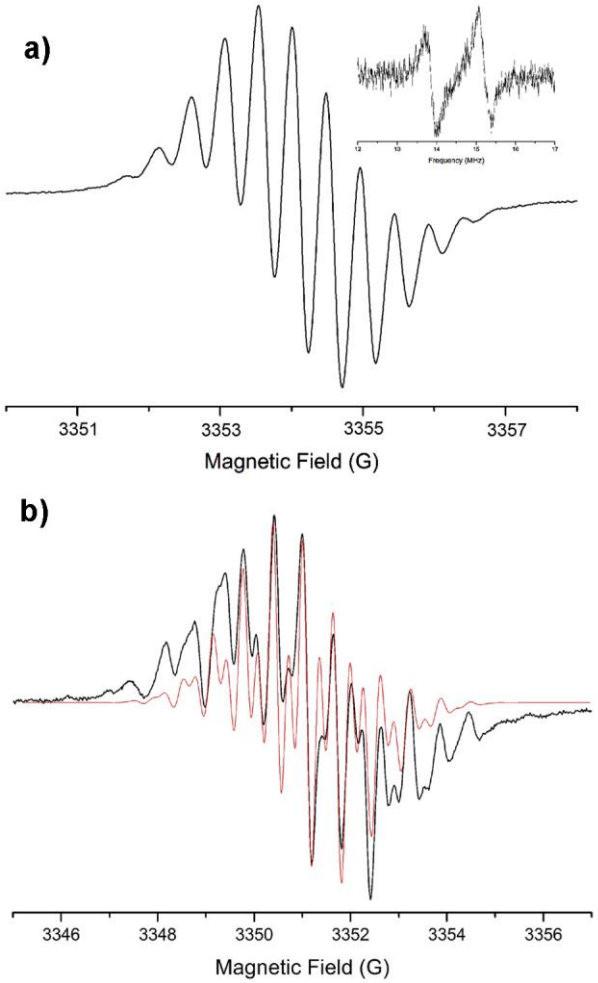

Figure 27. **a**) EPR spectrum of [*cis*-**17**]$^{+\bullet}$ (CH_2Cl_2, (TBA)PF_6 0.2 M, E = +0.4 V *vs.* Ag/Ag^+, T = 300 K, ν = 9426 MHz); g_{iso} = 2.008, A_{iso} = 0.48 G. Inset: ENDOR ^{1}H of *cis*-**17** oxidized by 1 equiv. of $NOBF_4$ in CH_2Cl_2; T=270 K, ν = 9593 MHz, A_{iso} = 1.32 MHz; **b**) Experimental (black) and simulated (red) EPR spectra of [*cis*-**21**]$^{+\bullet}$ (CH_2Cl_2, (TBA)PF_6 0.2 M, E = +0.45 V *vs.* Ag/Ag^+, T = 300 K, ν = 9426 MHz); g_{iso} = 2.010, A_{iso} ($^1H_{Me}$) = 0.62 G, A_{iso} (^{31}P) = 0.37 G. Adapted with permission from ref. [63]; Copyright 2009, American Chemical Society.

A similar spectrum was obtained by chemical oxidation with one equivalent of $NOBF_4$. Worth noting is the absence of a coupling with the phosphorous atoms indicating that no spin density is carried by the phosphine bridges, in agreement with the results on the diphosphine ligand (*o*-DMTTF)$(PPh_2)_2$.[47] DFT calculations provided an equilibrium geometry of [*cis*-**17**]$^{+\bullet}$ with a boat conformation of the central ring, the phenyl substituents in pseudo-equatorial positions (*exo*/*exo*) and a SOMO delocalized over both TTF units with no contribution of the P atoms.[63] Further oxidation with a second equivalent of $NOBF_4$ or at higher potentials corresponding to the generation of the dication [*cis*-**17**]$^{2+}$ afforded in a reversible manner a much more complex spectrum which could not be accurately simulated, yet demonstrating the radical nature of the dication. Electrocrystallization of *cis*-**17** in the presence of $(TBA)_2Mo_6O_{19}$ lead to the formation of a crystalline radical cation salt formulated as $[(DMTTF\text{-}PhPO)_2]_2(Mo_6O_{19})\bullet 2H_2O$, thus containing the radical cation of the bis(phosphine-oxide). In the solid state the TTF units are not equivalent, as one of them (S3-S4) is highly folded along the inner S3···S3

axis, while the other one (S1-S2) is planar, the donor molecule having crystallized on a mirror plane passing through the central C=C bonds (Figure 28).[61]

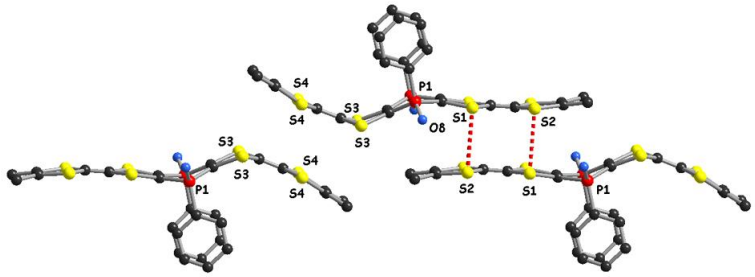

Figure 28. Packing of donors in the solid state structure of (*cis*-**17**-O_2)$_2$(Mo_6O_{19})•2H_2O. The short intermolecular S1···S2 contacts (3.36 Å) are highlighted in red dotted line. H atoms have been omitted.

When considering the intermolecular S···S distances, only S1···S2 (3.36 Å) is particularly short, being established between the flat TTF units interacting in a ring-over-ring fashion, while the shortest S···S distance between the folded TTFs (3.79 Å) exceeds the sum on the van der Waals radii. Thus one can hypothesize that in this radical cation of *cis*-**17** bis(oxide) charge ordering takes place, with the flat TTFs being charge rich and folded TTFs charge poor. Then, the former overlap through the S1···S2 contacts forming strong dimers. It is therefore not surprising that this material is a poor semiconductor, with a room temperature conductivity $\sigma < 10^{-5}$ S cm^{-1}. The formation of the phosphine oxide of *cis*-**17** upon electrocrystallization highlighted the reactivity of the phosphorous atoms. In a further study *cis*/*trans* mixtures of **17** were subjected to the formation of bis-sulfides **19** and bimetallic $M(CO)_5$ (M = Mo, W) complexes **20** and **21**, respectively (Figure 29).[63]

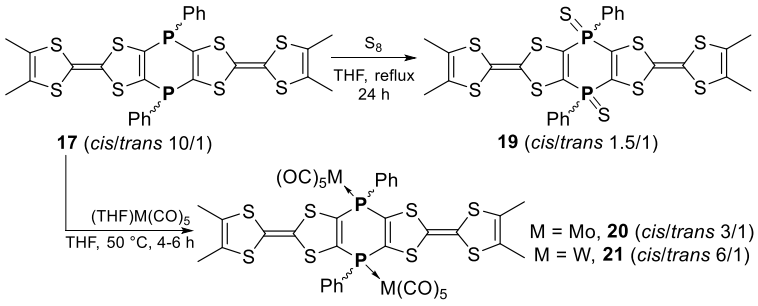

Figure 29. Reactivity of **17**. Adapted with permission from ref. [63]; Copyright 2009, American Chemical Society.

Although suitable single crystals for X-ray diffraction analysis were obtained for *trans*-**19** and *trans*-**20** from the respective *cis*/*trans* mixtures, only the isomers of **21** could be efficiently separated by column chromatography and crystallized. The X-ray analysis confirmed the formation of bimetallic complexes with octahedral $W(CO)_5P$ fragments. In *cis*-**21** the central ring adopts a boat conformation, yet the folding along the P···P axis is now only 14.5°, which is much weaker than in the free ligand (*vide supra*) (Figure 30).

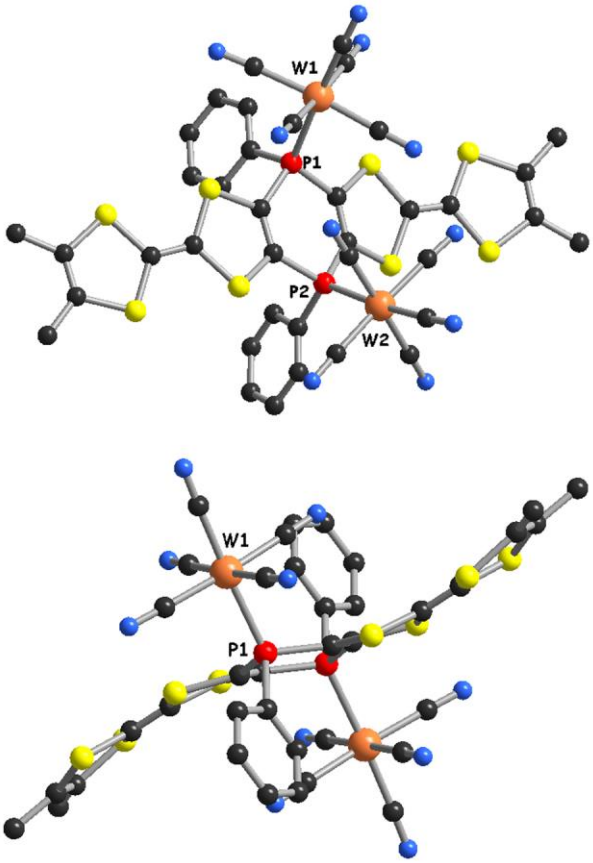

Figure 30. Solid state structures of *cis*-**21** (top) and *trans*-**21** (bottom). H atoms have been omitted.

In *trans*-**21** the 1,4-diphosphinine ring is slightly distorted within a chair conformation. In both isomers the Ph substituents adopt pseudo-equatorial orientations (*exo*/*exo*) (Figure 30). The isolation of **20** and **21**, which are to date the only metal complexes of such dimers, demonstrates the ability of these rigid electroactive diphosphines to coordinate transition metal fragments and thus opens the way towards the preparation of more complex architectures including coordination polymers. Note that the electrochemical behavior of **17** was not strongly affected upon formation of **19**-**21**, since stepwise reversible oxidation into radical cations and then dications were observed for all compounds at slightly more anodic potentials.[63] The radical cation species of *cis*-**21** was electrochemically generated and investigated by EPR (Figure 27b). While the spectrum was more complex than the one of the free ligand *cis*-**17**, it was nevertheless informative on the extended delocalization of the radical on both TTF units at the EPR time scale. In order to accurately simulate the spectrum, besides an hyperfine coupling of 0.62 G with twelve equivalent protons, a coupling of 0.37 G with two equivalent phosphorous nuclei had to be considered. This feature suggests possible modulation of the spin density upon coordination of the phosphines.

4. Conclusions

As outlined across this account, the connection of at least two TTF units through heteroatom based bridges provides multi-redox systems, with close vicinity of the electroactive units, hardly obtainable with other strategies. The relatively large choice of possible heteroatoms, i.e. groups XIV-XVI, of different nature, valence, bonding properties and reactivity which can be used as bridges, as well as the number of such bridges, provided a collection of flexible and rigid bis(TTF) precursors. Moreover, thanks to the availability and suitable reactivity of phosphorous tris(halides) several $P(TTF)_3$ phosphines have been described, yet the number of such tris(TTFs) is very limited compared to the bis(TTFs) compounds. To date no rigid tris(TTF) containing two heteroatom bridges has been reported, making it one of the possible challenges to address in the future. Two distinct periods in the development of these precursors have been underlined. The first one covers the decade from the end of the eighties till the end of the nineties with a very active research especially from the groups of Becker/Bernstein and Bryce on flexible and rigid derivatives containing chalcogen bridges $X(TTF)_2$ and $X_2(TTF)_2$ (X = S, Se, Te), together with the pioneering work of Fourmigué on bis- and tris(TTF) phosphines. Then after a gap of several years a renewal of the activity has been started in 2004 with our own research on rigid bis(TTF) phosphines, followed by reports dealing with derivatives containing group XIV (Si, Ge, Sn) and XV (P, Sb) bridges, coming from a few groups including ours. In spite of the obvious interest of such flexible and rigid bis(TTF) precursors, very few conducting materials have been prepared. This review, besides the objective to bring into light these attractive precursors, has also the ambition to motivate further endeavor towards the preparation of new such derivatives and their use towards conducting materials with original architectures and functionalities in which the heteroatom bridges play an active role. The inventory of the precursors shows that, with the exception of compound **15** based on tetraselenafulvalene (TSF), only TTF has been used as electroactive unit. There is clearly room for improvement in the direction of using more extensively TSF, although its functionalization is more challenging. Regarding the bridging heteroatom, the use of boron could open up yet unexplored possibilities. The potential offered by the rigid diphosphines such as **17** should be further developed as well. Moreover, an aspect which was not addressed at all within these families of precursors is the introduction of stereogenic centers, as recent reports highlighted the influence of chirality on the conducting properties of TTF based materials.[64,65]

Acknowledgements

This research was supported by the CNRS and the University of Angers. I would like to warmly thank all my co-workers and collaborators on this topic, especially Marc Fourmigué and Ion Danila, for their outstanding contributions.

Notes and references

[1] J.-I. Yamada, *TTF Chemistry: Fundamentals and Applications of Tetrathiafulvalene*, Springer-Verlag, Berlin and Heidelberg, **2004**.

[2] T. Ishiguro, K. Yamaji, G. Saito, *Organic Superconductors*, Heidelberg, Springer-Verlag, **1998**.

[3] N. Avarvari, J. D. Wallis, *J. Mater. Chem.* **2009**, *19*, 4061–4076.

[4] T. Otsubo, Y. Aso, K. Takimiya, *Adv. Mater.* **1996**, *8*, 203–211.

[5] M. Iyoda, M. Hasegawa, Y. Miyake, *Chem. Rev.* **2004**, *104*, 5085–5113.

[6] M. Iyoda, Y. Kuwatani, N. Ueno, M. Oda, *J. Chem. Soc., Chem. Commun.* **1992**, 158–159.

[7] T. Otsubo, Y. Kochi, A. Bitoh, F. Ogura, *Chem. Lett.* **1994**, 2047–2050.

[8] A. Izuoka, R. Kumai, T. Sugawara, *Chem. Lett.* **1992**, 285–288.

[9] N. Thorup, G. Rindorf, K. Lerstrup, K. Bechgaard, *Synth. Met.* **1991**, *41–43*, 2423–2426.

[10] C. Mézière, M. Fourmigué, E. Canadell, R. Clérac, K. Bechgaard, P. Auban-Senzier, *Chem. Mater.* **2000,** *12,* 2250–2256.

[11] A. Dolbecq, K. Boubekeur, P. Batail, E. Canadell, P. Auban-Senzier, C. Coulon, K. Lerstrup, K. Bechgaard, *J. Mater. Chem*. **1995**, *5*, 1707–1718.

[12] P. Wolf, H. Naarmann, K. Müllen, *Angew. Chem., Int. Ed. Engl.* **1988**, *27*, 288–289.

[13] M. L. Kaplan, R. C. Haddon, F. Wudl, *J. Chem. Soc., Chem. Commun.* **1977**, 388–389.

[14] M. Iyoda, M. Fukuda, M. Yoshida, S. Sasaki, *Chem. Lett.* **1994**, 2369–2372.

[15] A. González, J. L. Segura, N. Martín, *Tetrahedron Lett*. **2000**, *41*, 3083–3086.

[16] F. Riobé, N. Avarvari, P. Grosshans, H. Sidorenkova, T. Berclaz, M. Geoffroy, *Phys. Chem. Chem. Phys.* **2010**, *12*, 9650–9660.

[17] F. Riobé, P. Grosshans, H. Sidorenkova, M. Geoffroy, N. Avarvari, *Chem. Eur. J.* **2009**, *15*, 380–387.

[18] F. Pop, F. Riobé, S. Seifert, T. Cauchy, J. Ding, N. Dupont, A. Hauser, M. Koch, N. Avarvari, *Inorg. Chem.* **2013**, *52*, 5023–5034.

[19] K. Lahlil, A. Moradpour, C. Bowlas, F. Menou, P. Cassoux, J. Bonvoisin, J.-P. Launay, G. Dive, D. Dehareng, *J. Am. Chem. Soc.* **1995**, *117*, 9995–10002.

[20] D. Lorcy, N. Bellec, M. Fourmigué, N. Avarvari, *Coord. Chem. Rev.* **2009**, *253*, 1398–1438.

[21] S. Perruchas, N. Avarvari, D. Rondeau, E. Levillain, P. Batail, *Inorg. Chem.* **2005**, *44*, 3459–3465.

[22] G. Prabusankar, Y. Molard, S. Cordier, S. Golhen, Y. Le Gal, C. Perrin, L. Ouahab, S. Kahlal, J.-F. Halet, *Eur. J. Inorg. Chem.* **2009**, 2153–2161.

[23] M. Yuan, B. Ülgüt, M. McGuire, K. Takada, F. J. DiSalvo, S. Lee, H. Abruña, *Chem. Mater.* **2006,** *18,* 4296–4306.

[24] N. Avarvari, K. Kiracki, R. Llusar, V. Polo, I. Sorribes, C. Vicent, *Inorg. Chem.* **2010**, *49*, 1894–1904.

[25] J. O. Jeppesen, M. B. Nielsen, J. Becher, *Chem. Rev.* **2004**, *104*, 5115–5131.

[26] M. Fourmigué, P. Batail, *Chem. Commun.* **1991**, 1370–1372.

[27] F. Gerson, A. Lamprecht, M. Fourmigué, *J. Chem. Soc. Perkin Trans. 2* **1996**, 1409–1414.

[28] S. Perruchas, N. Avarvari, M. Fourmigué, *C. R. Chimie* **2004**, *7*, 895–899.

[29] J. Y. Becker, J. Bernstein, S. Bittner, J. A. R. P. Sarma, L. Shahal, *Tetrahedron Lett.* **1988**, *29*, 6177–6180.

[30] J. Y. Becker, J. Bernstein, M. Dayan, L. Shahal, *J. Chem. Soc., Chem. Commun.* **1992**, 1048–1049.

[31] M. R. Bryce, G. Cooke, A. S. Dhindsa, D. J. Ando, M. B. Hursthouse, *Tetrahedron Lett.* **1992**, *33*, 1783–1786.

[32] P. Leriche, M. Giffard, A. Riou, J.-P. Majani, J. Cousseau, M. Jubault, A. Gorgues, J. Becher *Tetrahedron Lett.* **1996**, *37*, 5115–5118.

[33] J. D. Martin, E. Canadell, J. Y. Becker, J. Bernstein, *Chem. Mater.* **1993**, *5*, 1199–1203.
[34] J. Y. Becker, J. Bernstein, S. Bittner, Y. Giron, E. Harlev, L. Kaufmanorenstein, D. Peleg, L. Shahal, S. S. Shaik, *Synth. Met.* **1991**, *41–43*, 2523–2528.
[35] J. Y. Becker, J. Bernstein, M. Dayan, A. Ellern, L. Shahal, *Adv. Mater.* **1994**, *6*, 758–761.
[36] M. Fourmigué, Y.-S. Huang, *Organometallics* **1993**, *12*, 797–802.
[37] A. Hameau, F. Guyon, M. Knorr, C. Däschlein, C. Strohmann, N. Avarvari, *Dalton Trans.* **2008**, 4866–4876.
[38] A. Bondi, *J. Phys. Chem.* **1964**, *68*, 441–451.
[39] M. A. Spackman, *J. Chem. Phys.* **1986**, *85*, 6579–6586.
[40] M. Ashizawa, H. M. Yamamoto, A. Nakao, R. Kato, *Tetrahedron Lett.* **2006**, *47*, 8937–8941.
[41] S. S. Kuduva, N. Avarvari, M. Fourmigué, *J. Chem. Soc. Dalton Trans*. **2002**, 3686–3690.
[42] A. J. Ashe, III, W. Butler, T. R. Diephouse, *J. Am. Chem. Soc.* **1981**, *103*, 207–209.
[43] N. Avarvari, E. Faulques, M. Fourmigué, *Inorg. Chem*. **2001**, *40*, 2570–2577.
[44] N. Avarvari, M. Fourmigué, *Organometallics* **2003**, *22*, 2042–2049.
[45] N. Avarvari, D. Martin, M. Fourmigué, *J. Organomet. Chem.* **2002,** *643-644*, 292–300.
[46] T. Devic, P. Batail, M. Fourmigué, N. Avarvari, *Inorg. Chem.* **2004**, *43*, 3136–3141.
[47] C. Gouverd, F. Biaso, L. Cataldo, T. Berclaz, M. Geoffroy, E. Levillain, N. Avarvari, M. Fourmigué, F.-X. Sauvage, C. Wartelle, *Phys. Chem. Chem. Phys*. **2005**, *7*, 85–93.
[48] N. Avarvari, M. Fourmigué, *Chem. Commun.* **2004**, 1300–1301.
[49] D. Rondeau, S. Perruchas, N. Avarvari, P. Batail, K. Vekey, *J. Mass. Spectr.* **2005**, *40*, 60–65.
[50] N. Avarvari, M. Fourmigué, *Chem. Commun.* **2004**, 2794–2795.
[51] C. Wang, A. Ellern, J. Y. Becker, J. Bernstein, *Adv. Mater.* **1995**, *7*, 644–646.
[52] E. Aqad, J. Y. Becker, J. Bernstein, A. Ellern, V. Khodorkovsky, L. Shapiro, *J. Chem. Soc., Chem. Commun.* **1994**, 2775–2776.
[53] L. M. Goldenberg, V. Yu. Khodorkovsky, J. Y. Becker, M. R. Bryce, M. C. Petty, *J. Mater. Chem.* **1995**, *5*, 191–192.
[54] H. Yamochi, G. Saito, *Synth. Met.* **1997**, *85*, 1467–1468.
[55] C. Wang, A. Ellern, V. Khodorkovsky, J. Y. Becker, J. Bernstein, *J. Chem. Soc., Chem. Commun.* **1994**, 2115–2116.
[56] C. Wang, A. Ellern, J. Y. Becker, J. Bernstein, *Tetrahedron Lett.* **1994**, *35*, 8489–8492.
[57] E. Ojima, H. Fujiwara, H. Kobayashi, A. Kobayashi, *Adv. Mater.* **1999**, *11*, 1527–1530.
[58] F. Biaso, M. Geoffroy, E. Canadell, P. Auban-Senzier, E. Levillain, M. Fourmigué, N. Avarvari, *Chem. Eur. J.* **2007**, *13*, 5394–5400.
[59] M. Shirai, M. Hasegawa, H. Sato, Y. Mazaki, *Chem. Lett.* **2014**, *43*, 592–594.
[60] M. Hasegawa, M. Shirai, Y. Mazaki, *Eur. J. Inorg. Chem.* **2018**, 4084–4092.
[61] N. Avarvari, M. Fourmigué, *Chem. Commun.* **2004**, 2794–2795.
[62] I. Danila, N. Avarvari, *C. R. Chimie* **2010**, *13*, 1227–1232.
[63] I. Danila, F. Biaso, H. Sidorenkova, M. Geoffroy, M. Fourmigué, E. Levillain, N. Avarvari, *Organometallics* **2009**, *28*, 3691–3699.
[64] F. Pop, P. Auban-Senzier, E. Canadell, G. L. J. A. Rikken, N. Avarvari, *Nat. Commun.* **2014**, *5*, 3757.
[65] F. Pop, N. Zigon, N. Avarvari, *Chem. Rev.* **2019**, *119*, 8435–8478.

Table of Contents Entry

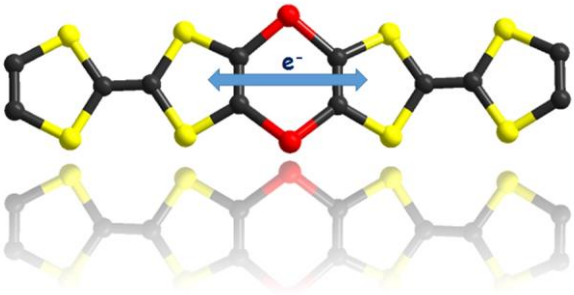

Flexible and rigid bis(TTF) precursors containing heteroatom based bridges are reviewed together with their charge transfer complexes and radical cation salts with a special focus on their crystalline structures and electronic properties.

Keywords: Tetrathiafulvalene; Heteroatoms; Mixed valence; Charge transfer complexes; Conducting materials

Key Topic: Electronic communication; Heteroatom bridges